Model-Based Automotive Control Design Using Port-Hamiltonian Systems

Siyuan Dai and Xenofon Koutsoukos*

Abstract— **Model-based design is an important tool for cyber-physical systems (CPS) that efficiently connects all development phases of control software and ensures desirable system performance. However, the increased complexity of CPS caused by interactions between components creates challenges for the implementation of model-based design. In this paper, we present a modeling framework for the model-based design toolchain which uses port-Hamiltonian systems (PHS) to model CPS components and interactions. In this framework, passivity-based control methods are used to design controllers and compose them through Dirac structures. We evaluate the modeling framework using an automotive control system and present simulation results to demonstrate the effectiveness of the framework.**

I. Introduction

CPS are engineering systems characterized by complex integrations of physical and computational domains over communication networks [10]. Automotive systems are examples of CPS in which various physical components are controlled by electronic control units (ECUs) communicating over networks. Rigorous engineering methods are essential for designing control systems that can be integrated with the vehicle dynamics to achieve predictable and correct behavior. Model-based control design is crucial for automotive systems and creates a common framework during the design stage of the development process.

In our previous work, we developed a model-based design toolchain for automotive control systems which integrates control design, software implementation, and deployment on a hardware-in-the-loop simulation platform [5]. This toolchain provides a means to design and implement control software on a realistic platform while focusing on the interactions that manifest during the integration stage of development.

Despite its benefits, the model-based design toolchain faces challenges caused by interactions between components, which increases the complexity of CPS. Problems from the integration of components are often discovered late in the development cycle, leading to costly ramifications of the designs. As modern CPS expand in complexity, a modeling framework which can effectively capture their components and interactions becomes increasingly necessary.

This paper presents a compositional modeling framework based on PHS. The framework enables the use of passivity-based control methods to design individual controllers and connect them through Dirac structures [7]. Additionally, the framework is applicable to systems that contain nonlinear and hybrid dynamics. We present a case study where the dynamics of a vehicle system is decomposed into its longitudinal and lateral dynamics interacting through a Dirac structure. We then use the framework to design a speed and steering control system that interact with each other to achieve autonomous driving. We validate the vehicle dynamics model by comparing the passivity index values of the PHS model and a realistic CarSim vehicle model [1]. We evaluate the control design using simulations to show that the closed-loop system behaves correctly.

The theory of PHS is presented in detail in [4]. PHS have significant implications for passivity, which has been studied extensively for control design and analysis of nonlinear systems [6]. An important property of PHS is compositionality, where component PHS compose with each other through the interaction ports of their respective Dirac structures. The result of composing two PHS is another PHS, which provides a compositional framework for modeling complex physical lumped-parameter systems [2].

The rest of the paper is organized as follows. Section II presents the related work on model-based design. Section III applies the PHS modeling framework to the dynamics of an automotive system. Section IV applies the PHS modeling framework to the control portion of the automotive system. Section V presents the validation of the vehicle dynamics and control system using simulation results. The paper is concluded in Section VI.

II. Model-Based Design

Model-based design of CPS is an active research area where a large amount of work is being done to address the various challenges caused by the heterogeneity of the different layers of CPS [10]. We created a toolchain to integrate the components of control design from Matlab/Simulink with the aspects of software deployment such as scheduling, discretization, and quantization with

*Siyuan Dai and Xenofon Koutsoukos are with the Department of Electrical Engineering and Computer Science, Vanderbilt University, Nashville, TN, USA {siyuan.dai, xenofon.koutsoukos}@vanderbilt.edu

978-1-4673-7178-0/15/$31.00 ©2015 IEEE

a primary application to automotive control systems [5]. The toolchain is designed using an embedded software design environment called Embedded Systems Modeling Language (ESMoL) [8]. The toolchain is evaluated over a hardware-in-the-loop experimental platform over a time-triggered communication network which guarantees that the whole process is reliable, predictable, and robust to disturbances.

The first step of the model-based design toolchain is designing and modeling the controller for a particular function in Matlab/Simulink and using simulations to test and verify the correctness of the system. The approach we developed in this paper focuses on this step of the model-based design process by modeling both the controller and plant as PHS, and using passivity-based design methods to ensure correct behavior of the overall system. PHS provide an effective way of characterizing the interactions presented in the CPS and is also able to model nonlinearities and hybrid dynamics. The resulting control design model from this approach can then be imported into ESMoL and used for subsequent phases of the model-based design process.

The remaining design steps consist of importing the control designs into ESMoL, specifying the logical software architecture, defining the hardware platform, deploying the model, specifying the timing behavior of the system, flattening the model for analysis, scheduling the tasks, and implementing on the platform for testing [5].

III. System Model

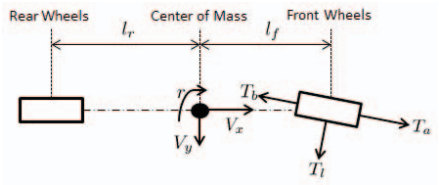

Fig. 1. Free-body diagram of the vehicle dynamics

Figure 1 shows a free-body diagram of the vehicle dynamics; the vehicle is front-wheel drive, resulting in the input forces from throttle and brake being applied to the front wheels on the diagram. The longitudinal input force from the throttle, $T_a = C_a\theta_a$, is a function of the throttle valve angle θ_a and the experimental throttle constant C_a. The longitudinal input force from the brakes, $T_b = C_bP_b$, is a function of the braking pressure P_b and the experimental braking constant C_b. The lateral input force from the steering, $T_l = 2C_f\delta$, is a function of the steering angle δ and the cornering stiffness of the front wheels C_f. The longitudinal velocity, lateral velocity, and yaw rate, are represented by V_x, V_y, and r, respectively. Interactions between the longitudinal and lateral dynamics can be derived by analysis of the free-body diagram [9].

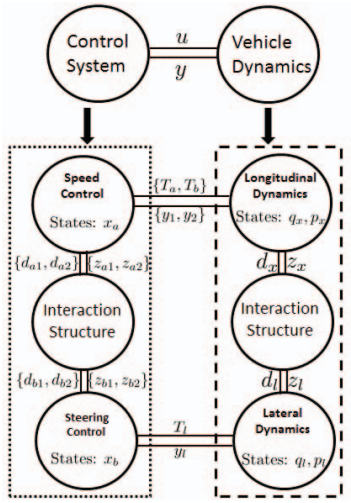

Fig. 2. PHS representation of the high level system model

Using PHS, we model the longitudinal dynamics, the lateral dynamics, and their interactions in a compositional way, shown in Figure 2. The vehicle dynamics model is decomposed into a longitudinal dynamics component, a lateral dynamics component, and an interaction structure. The longitudinal dynamics contain two control ports (T_a, y_1) and (T_b, y_2) and an interaction port (d_x, z_x). The state variables are the longitudinal momentum p_x and the longitudinal displacement q_x. The outputs of the control ports y_1 and y_2 are V_x and $-V_x$, respectively. The x-component of the lateral force affecting longitudinal motion is represented by d_x and its power-conjugate is represented by z_x. The lateral dynamics contain a control port (T_l, y_l) and an interaction port (d_l, z_l). The state variables are $q_l = \begin{bmatrix} q_y & q_r \end{bmatrix}^\mathsf{T}$ and $p_l = \begin{bmatrix} p_y & p_r \end{bmatrix}^\mathsf{T}$, where p_y is the lateral momentum, p_r is the angular momentum, q_y is the lateral displacement, and q_r is the angular displacement. The output of the control port y_l is $V_y + l_f r$. The y-component of the longitudinal force applied to the center of mass is represented by d_l and its power-conjugate is represented by z_l.

Using PHS, we design a control system for autonomous driving which controls T_a, T_b, and T_l. The objective of the control system is to maintain a desired speed V_d and lateral displacement q_d. The control system model consists of a speed control component, a steering control component, and an interaction structure. The speed control shares the two control ports with the longitudinal dynamics and contains two interaction ports (d_{a1}, z_{a1}) and (d_{a2}, z_{a2}); its state variables $x_a = \begin{bmatrix} x_{at} & x_{ab} \end{bmatrix}^\mathsf{T}$ are derived using the desired speed, where

$x_{at} = \int_{t_0}^{t}(V_x - V_d)d\tau$ and $x_{ab} = \int_{t_0}^{t}(V_d - V_x)d\tau$. The steering control shares the control port with the lateral dynamics and contains two interaction ports (d_{b1}, z_{b1}) and (d_{b2}, z_{b2}); its state variable $x_b = q_y - q_d$ is derived using the desired lateral displacement.

A. Longitudinal Dynamics

The longitudinal dynamics has the following Hamiltonian function:

$$H_x(q_x, p_x) = \frac{1}{2m}p_x^2 + U_x(q_x),$$

where m represents the mass of the vehicle and $U_x(q_x)$ represents the potential energy. Consider the input-state-output PHS:

$$\begin{cases} \dot{x} &= [J(x) - R(x)]\frac{\partial H}{\partial x} + G(x)u + K(x)d \\ y &= G^{\mathsf{T}}(x)\frac{\partial H}{\partial x} \\ z &= K^{\mathsf{T}}(x)\frac{\partial H}{\partial x}, \end{cases} \tag{1}$$

where $J(x) \in \mathbb{R}^{n\times n}$ is a skew symmetric interconnection matrix, $R(x) \in \mathbb{R}^{n\times n}$ is a symmetric positive-semidefinite damping matrix, inputs/outputs $(u, y) \in \mathbb{R}^{m\times m}$, and interactions $(d, z) \in \mathbb{R}^{j\times j}$ $(m, j \le n)$. The longitudinal dynamics is modeled in the form of (1):

$$\begin{cases} \begin{bmatrix}\dot{q}_x \\ \dot{p}_x\end{bmatrix} &= \begin{bmatrix}0 & 1 \\ -1 & -R_x\end{bmatrix}\begin{bmatrix}\frac{\partial H_x}{\partial q_x} \\ \frac{\partial H_x}{\partial p_x}\end{bmatrix} + \begin{bmatrix}0 \\ G_x\end{bmatrix}u_x + \begin{bmatrix}0 \\ 1\end{bmatrix}d_x \\ y_x &= \begin{bmatrix}0 & G_x^{\mathsf{T}}\end{bmatrix}\begin{bmatrix}\frac{\partial H_x}{\partial q_x} & \frac{\partial H_x}{\partial p_x}\end{bmatrix}^{\mathsf{T}} \\ z_x &= \begin{bmatrix}0 & 1\end{bmatrix}\begin{bmatrix}\frac{\partial H_x}{\partial q_x} & \frac{\partial H_x}{\partial p_x}\end{bmatrix}^{\mathsf{T}}, \end{cases} \tag{2}$$

where $u_x = \begin{bmatrix}T_a & T_b\end{bmatrix}^{\mathsf{T}}$, $G_x = \begin{bmatrix}1 & -1\end{bmatrix}$, $R_x = am + bp_x + \frac{cm^2}{p_x}$, a represents the tire rolling friction constant, b represents the air resistance constant, and c represents the static friction force.

B. Lateral Dynamics

The lateral dynamics has the following Hamiltonian function:

$$H_l(q_y, q_r, p_y, p_r) = \frac{1}{2m}p_y^2 + \frac{1}{2I}p_r^2 + U_l(q_y, q_r),$$

where I represents the moment of inertia of the vehicle and $U_l(q_y, q_r)$ represents the potential energy. The lateral dynamics is modeled in the form of (1):

$$\begin{cases} \begin{bmatrix}\dot{q}_l \\ \dot{p}_l\end{bmatrix} &= \begin{bmatrix}0 & E \\ -E & -R_l\end{bmatrix}\begin{bmatrix}\frac{\partial H_l}{\partial q_l} \\ \frac{\partial H_l}{\partial p_l}\end{bmatrix} + \begin{bmatrix}0 \\ G_l\end{bmatrix}T_l + \begin{bmatrix}0 \\ K_l\end{bmatrix}d_l \\ y_l &= \begin{bmatrix}0 & G_l^{\mathsf{T}}\end{bmatrix}\begin{bmatrix}\frac{\partial H_l}{\partial q_l} & \frac{\partial H_l}{\partial p_l}\end{bmatrix}^{\mathsf{T}} \\ z_l &= \begin{bmatrix}0 & K_l^{\mathsf{T}}\end{bmatrix}\begin{bmatrix}\frac{\partial H_l}{\partial q_l} & \frac{\partial H_l}{\partial p_l}\end{bmatrix}^{\mathsf{T}}, \end{cases} \tag{3}$$

$$R_l = \begin{bmatrix}\frac{W_1}{V_x} & \frac{W_2}{V_x} \\ \frac{W_2}{V_x} & \frac{W_3}{V_x}\end{bmatrix},$$

where E is the identity matrix, $G_l = \begin{bmatrix}1 & l_f\end{bmatrix}^{\mathsf{T}}$ and $K_l = \begin{bmatrix}1 & 0\end{bmatrix}^{\mathsf{T}}$. The parameter constants of R_l are $W_1 = 2C_f + 2C_r$, $W_2 = 2C_f l_f - 2C_r l_r$, and $W_3 = 2C_f l_f^2 + 2C_r l_r^2$, where C_r is the cornering stiffness of the rear wheels.

C. Vehicle Dynamics Interactions

The interaction between the longitudinal and lateral dynamics is a mapping of velocity to force, which indicates a gyrator relationship. The gyrator ratio must have units of kg/s which is represented by multiplying the mass of the vehicle with the yaw rate. The interaction structure is modeled as a Dirac structure modulated by the angular momentum p_r:

$$\begin{bmatrix}d_x \\ d_l\end{bmatrix} = \begin{bmatrix}0 & -\frac{mp_r}{I} \\ -\frac{mp_r}{I} & 0\end{bmatrix}\begin{bmatrix}z_x \\ z_l\end{bmatrix}. \tag{4}$$

The Hamiltonian function of the composed longitudinal and lateral dynamics is $H(q, p) = H_x + H_l$. Composition of (2) and (3) through (4) results in the following nonlinear PHS:

$$\begin{cases} \begin{bmatrix}\dot{q} \\ \dot{p}\end{bmatrix} &= \begin{bmatrix}0 & E \\ -E & -R\end{bmatrix}\begin{bmatrix}\frac{\partial H}{\partial q} \\ \frac{\partial H}{\partial p}\end{bmatrix} + \begin{bmatrix}0 \\ G\end{bmatrix}u \\ y &= \begin{bmatrix}0 & G^{\mathsf{T}}\end{bmatrix}\begin{bmatrix}\frac{\partial H}{\partial p} \\ \frac{\partial H}{\partial p}\end{bmatrix}, \end{cases} \tag{5}$$

$$R = \begin{bmatrix}R_x & \frac{mp_r}{I} & 0 \\ \frac{mp_r}{I} & \frac{mW_1}{p_x} & \frac{mW_2}{p_x} \\ 0 & \frac{mW_2}{p_x} & \frac{mW_3}{p_x}\end{bmatrix}, G = \begin{bmatrix}G_x & 0 \\ 0 & G_l\end{bmatrix},$$

where $q = \begin{bmatrix}q_x & q_l\end{bmatrix}^{\mathsf{T}}$, $p = \begin{bmatrix}p_x & p_l\end{bmatrix}^{\mathsf{T}}$, $u = \begin{bmatrix}u_x & T_l\end{bmatrix}^{\mathsf{T}}$, and $y = \begin{bmatrix}y_x & y_l\end{bmatrix}^{\mathsf{T}}$. Interactions between the longitudinal and lateral dynamics are captured in R.

IV. Control Design and Analysis

A. Speed Control

We design the speed control to have the following Hamiltonian function:

$$H_a(x_a, s) = \frac{1}{2}(s_t k_{ti} x_{at}^2 + s_b k_{bi} x_{ab}^2),$$

where k_{ti} and k_{bi} are the gains of the Hamiltonian. The discrete variables $s = (s_t, s_b) \in \{0, 1\}$ are used to model the hybrid dynamics of throttling and braking. The switching dynamics are defined in (6), where h_+ and h_- are hysteresis constants introduced to prevent the system from rapidly alternating between accelerating and decelerating, and X_r and X_d are the relative distance between the two vehicles and the desired distance, respectively:

$$\begin{cases} (s_t, s_b) = (1, 0) \text{ for } V_d - y_1 \ge 0, X_r \ge h_+ X_d, \\ (s_t, s_b) = (0, 1) \text{ for } V_d - y_1 < 0, X_r < h_- X_d. \end{cases} \tag{6}$$

We design the speed control as an input-state-output PHS with direct-feedthrough [11]:

$$\begin{cases} \dot{x} &= [J(x) - R(x)]\frac{\partial H}{\partial x} + G(x)u + K_1(x)d_1 \\ y &= G^{\mathsf{T}}(x)\frac{\partial H}{\partial x} + [M(x) + S(x)]u + K_2(x)d_2 \\ z &= \begin{bmatrix} K_1(x)^{\mathsf{T}} & 0 \\ 0 & K_2(x)^{\mathsf{T}} \end{bmatrix} \begin{bmatrix} \frac{\partial H}{\partial x} \\ u \end{bmatrix}, \end{cases} \tag{7}$$

where $M(x) \in \mathbb{R}^{m \times m}$ is a skew symmetric interconnection matrix and $S(x) \in \mathbb{R}^{m \times m}$ is a symmetric positive-semidefinite damping matrix. We design the speed control in the form of (7) because the feedthrough term helps to ensure zero steady-state error [4]:

$$\begin{cases} \dot{x}_a &= -R_a\frac{\partial H_a}{\partial x_a} + G_a y_x + K_{a1}d_{a1} \\ u_x &= G_a^{\mathsf{T}}\frac{\partial H_a}{\partial x_a} + S_a y_x + K_{a2}d_{a2} \\ \begin{bmatrix} z_{a1} \\ z_{a2} \end{bmatrix} &= \begin{bmatrix} K_{a1}^{\mathsf{T}} & 0 \\ 0 & K_{a2}^{\mathsf{T}} \end{bmatrix} \begin{bmatrix} \frac{\partial H_a}{\partial x_a} \\ y_x \end{bmatrix}, \end{cases} \tag{8}$$

where $K_{a1} = \begin{bmatrix} 1 & 0 \end{bmatrix}^{\mathsf{T}}$ and $K_{a2} = \begin{bmatrix} 1 & 0 \end{bmatrix}^{\mathsf{T}}$. The parameter matrices are denoted as:

$$R_a = \begin{bmatrix} s_t k_t & 0 \\ 0 & s_b k_b \end{bmatrix}, G_a = \begin{bmatrix} s_t P & 0 \\ 0 & s_b \end{bmatrix},$$

$$S_a = \begin{bmatrix} s_t k_{td} & 0 \\ 0 & s_b k_{bd} \end{bmatrix},$$

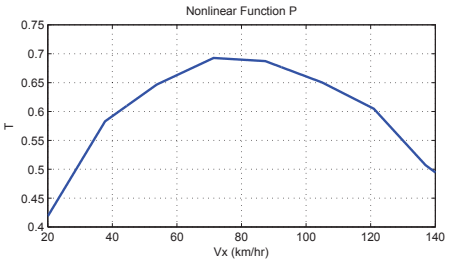

Fig. 3. Nonlinear Function P

where k_t and k_{td} are throttle control gains; k_b and k_{bd} are brake control gains. P is derived from the inverse engine map for the vehicle and is a mapping of the ratio of the acceleration force to the integrated difference of V_x and V_d (Figure 3) [5].

B. Steering Control

We design the steering control to have the following Hamiltonian function:

$$H_b(x_b) = \frac{1}{2}k_{si}x_b^2,$$

where k_{si} is the gain of the Hamiltonian. We design the steering control in the form of (7):

$$\begin{cases} \dot{x}_b &= y_l + d_{b1} \\ T_l &= \frac{\partial H_b}{\partial x_b} + k_{sd}y_l + d_{b2} \\ \begin{bmatrix} z_{b1} \\ z_{b2} \end{bmatrix} &= \begin{bmatrix} 1 & 0 \\ 0 & 1 \end{bmatrix} \begin{bmatrix} \frac{\partial H_b}{\partial x_b} \\ y_l \end{bmatrix}, \end{cases} \tag{9}$$

where k_{sd} is the steering control gain.

C. Controller Interactions

It can be seen from (5) that the inputs to the longitudinal dynamics (T_a and T_b) affect the lateral dynamics; similarly, the input to the lateral dynamics (T_l) affects the longitudinal dynamics. This can create problems such that at high speeds, actions by the speed control may interfere with the objective of the steering control. In order to alleviate this problem, we introduce an interaction structure so that the state variables and outputs of the speed control are affected by the state variable of the steering control, and vice versa. Similar to (4), the interaction structure of the control system is represented with the following Dirac structure:

$$\begin{bmatrix} d_{a1} \\ d_{a2} \\ d_{b1} \\ d_{b2} \end{bmatrix} = \begin{bmatrix} 0 & 0 & J_c & 0 \\ 0 & 0 & 0 & M_c \\ -J_c^{\mathsf{T}} & 0 & 0 & 0 \\ 0 & -M_c^{\mathsf{T}} & 0 & 0 \end{bmatrix} \begin{bmatrix} z_{a1} \\ z_{a2} \\ z_{b1} \\ z_{b2} \end{bmatrix}. \tag{10}$$

The parameters J_c and M_c define how the speed control and the steering control interact. The Hamiltonian function of the composed control system is denoted as $H_c = H_a + H_b$. Composition of (8) and (9) through (10) results in the following PHS representation:

$$\begin{cases} \dot{x} &= \begin{bmatrix} -R_a & J_s \\ -J_s^{\mathsf{T}} & 0 \end{bmatrix} \frac{\partial H_c}{\partial x} + \begin{bmatrix} G_a & 0 \\ 0 & 1 \end{bmatrix} y \\ u &= \begin{bmatrix} G_a^{\mathsf{T}} & 0 \\ 0 & 1 \end{bmatrix} \frac{\partial H_c}{\partial x} + \begin{bmatrix} S_a & M_s \\ -M_s^{\mathsf{T}} & k_{sd} \end{bmatrix} y, \end{cases} \tag{11}$$

where $J_s = \begin{bmatrix} J_c & 0 \end{bmatrix}^{\mathsf{T}}$, $M_s = \begin{bmatrix} M_c & 0 \end{bmatrix}^{\mathsf{T}}$, and $x = \begin{bmatrix} x_{at} & x_{ab} & x_b \end{bmatrix}^{\mathsf{T}}$.

D. Analysis

Theorem 1: The closed-loop system (11) is passive with respect to inputs y, outputs u, and Hamiltonian function $H_c = H_a + H_b$ if k_{ti}, k_{bi}, k_t, k_{td}, k_b, k_{bd}, k_{si}, $k_{sd} \geq 0$. Additionally, (11) will asymptotically stabilize the velocity V_x and the lateral position q_y to the desired velocity V_d and lateral position q_d, respectively.

Proof: Passivity of the composed control system is proven using the energy-balancing equation:

$$\begin{aligned} \frac{dH_c}{dt} &= \frac{\partial H_c}{\partial x}^{\mathsf{T}} \begin{bmatrix} -R_a & J_c \\ -J_c^{\mathsf{T}} & J_l \end{bmatrix} \frac{\partial H_c}{\partial x} + \frac{\partial H_c}{\partial x}^{\mathsf{T}} \begin{bmatrix} G_a & 0 \\ 0 & G_l \end{bmatrix} y \\ &\leq u^{\mathsf{T}}y - y^{\mathsf{T}} \begin{bmatrix} S_a & 0 \\ 0^{\mathsf{T}} & S_l \end{bmatrix} y. \end{aligned}$$

Passivity of the system is shown by the inequality $\frac{dH_c}{dt} \leq u^{\mathsf{T}} y$. Asymptotic stability of the closed-loop system is shown by combining (5) with (11). The PHS representation of the closed-loop system:

$$\left\{ \begin{bmatrix} \dot{q} \\ \dot{p} \\ \dot{x} \end{bmatrix} = \begin{bmatrix} -\tilde{M} & \tilde{M} & 0 \\ -\tilde{M}^{\mathsf{T}} & \tilde{J} & \tilde{K} \\ 0 & -\tilde{K}^{\mathsf{T}} & -\tilde{Q} \end{bmatrix} \begin{bmatrix} \frac{\partial \tilde{H}}{\partial q} \\ \frac{\partial \tilde{H}}{\partial p} \\ \frac{\partial \tilde{H}}{\partial x} \end{bmatrix} \right.,$$

where $\tilde{M}$, $\tilde{J}$, $\tilde{K}$, and $\tilde{Q}$ are defined as:

$$\tilde{M} = \text{diag}\left(\frac{1}{m}, \frac{1}{m}, \frac{1}{I}\right), \tilde{J} = \begin{bmatrix} 0 & \frac{M_c}{m} & 0 \\ -\frac{M_c}{m}^{\mathsf{T}} & 0 & 0 \\ 0 & 0 & 0 \end{bmatrix},$$

$$\tilde{K} = \begin{bmatrix} s_t k_{ti} P & 0 & 0 \\ 0 & s_b k_{bi} & 0 \\ 0 & 0 & \frac{k_{si}}{l_f} \end{bmatrix}, \tilde{Q} = \begin{bmatrix} s_t k_t & -\frac{J_c}{m} & 0 \\ \frac{J_c}{m}^{\mathsf{T}} & s_b k_b & 0 \\ 0 & 0 & 0 \end{bmatrix},$$

with a modified Hamiltonian function, $\tilde{H}(q, p, z)$:

$$\begin{aligned} \tilde{H} = \; & \tfrac{s_t k_{td}}{2m}(mV_d - p_x)^2 + \tfrac{s_b k_{bd}}{2m}(p_x - mV_d)^2 \\ & + \tfrac{1}{2m} p_y^2 + \tfrac{1}{2I} p_r^2 + \tfrac{k_{sd}}{2}(q_y - q_d)^2 \\ & + \tfrac{k_{ti}}{2} x_{at}^2 + \tfrac{k_{bi}}{2} x_{ab}^2 + \tfrac{k_{si}}{2} x_b^2, \end{aligned}$$

which we can use to verify that $\dot{\tilde{H}}$ is always less than or equal to zero and that $p_x = mV_d$ and $q_y = q_d$ at the boundary.

■

V. Evaluation

In this section, we present simulation results which test and verify (5) and (11). For validation of the PHS model we use a standard E-class sedan model in CarSim as a reference [1]. We select parameters for the vehicle dynamics model so that its passivity index values match that of the CarSim model. We validate the control design using simulations to show that the vehicle behaves correctly given changes in lead vehicle speed, road curvature, and slope of the road. After verifying the correctness of the control design and vehicle dynamics, we apply the model-based design toolchain on the control design to discretize, quantize, and account for other implementation effects while preserving passivity in preparation for deployment [5].

A. Model Validation

The CarSim model has inherent bounds on its inputs [1]. The throttle angle valve (θ_f) has a lower bound of 0 and an upper bound of 1.5. The brake pressure (P_b) has a lower bound of 0 and upper bound of 10. The steering angle (δ) has a lower bound of -480 and an upper bound of 480 [1]. Using these CarSim variable bound values we mathematically determine that T_a has a lower bound of 0 N and an upper bound of 3104 N; T_b has a lower bound of 0 N and an upper bound of 3715 N; T_l has a lower bound of -1200 N and an upper bound of 1200 N.

Passivity indexes allow a way to characterize a system by determining its excess or shortage of passivity [13]. By showing that the passivity indexes of the analytical models are similar to that of the CarSim model, we can conclude that the analytical models are reasonable approximations of the actual vehicle dynamics. Using the techniques demonstrated in [12], we determine that the passivity indexes of the CarSim model (ν_c, ρ_c) are (181, 0.6). We experimentally selected values for the vehicle model (Table I) so that the passivity indexes of the analytical model closely match that of the CarSim model. The CarSim model gives the mass ($m = 1650$) and the inertia ($I = 3234$). We determined that the passivity indexes of the analytical model (ν_a, ρ_a) are (177, 0.6), indicating that the analytical models are reasonable approximations of the CarSim model.

TABLE I

Table of vehicle parameter values

a	b	c	C_r	l_r	C_f	l_f
0.1	0.006	10	200	1.4	300	1.4

B. Control Validation

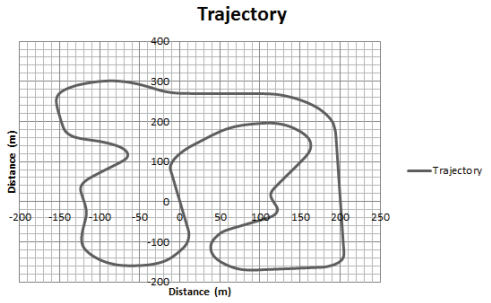

Fig. 4. Course trajectory for vehicle

Simulation of the closed-loop system consists of two minutes of running time in which the host vehicle follows a lead vehicle on a road with a trajectory shown in Figure 4. Table II shows the gain values of the controllers, which are computed using power-shaping stabilization [3]. We present simulation results for two control systems; in the first control system there are no interactions between the speed control and steering control, $J_c, M_c = 0$; in the second control system, the interaction gains are $J_c = 0.2$ and $M_c = -0.5$. Figure 5 shows the velocity of the lead vehicle and the host vehicle on the top subplot and the relative distance between

the two vehicles on the bottom subplot; Figure 6 shows the lateral displacement on the top subplot and the lateral acceleration on the bottom subplot. and Table III shows the various scenarios that appear during the simulation.

TABLE II

TABLE OF CONTROLLER GAINS

k_{ti}	k_{bi}	k_t	k_{td}	k_b	k_{bd}	k_{si}	k_{sd}
0.05	0.01	0.1	0.02	0.2	0.02	40	15

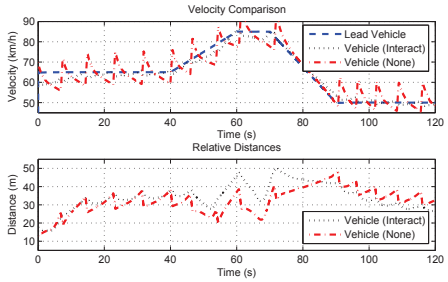

Fig. 5. Vehicle velocities and relative distances

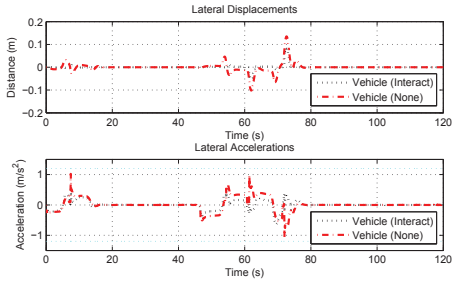

Fig. 6. Vehicle lateral accelerations and displacements

The simulation results indicate that the control system is able to keep to the objectives of speed control and steering control despite changes in the lead vehicle speed, slopes, and turns encountered by the host vehicle. For the results shown in Figure 5, the lack of interactions between the speed and steering control results in relatively large changes in speed; the addition of interactions results in a smoother velocity profile. Figure 6 also indicate better results for the case with interactions. Based on the simulation results, we determine that the maximum lateral acceleration $A_m \approx 1.2$ m/s^2; marking cyan dashed lines for A_m and $-A_m$ on the second subplots of Figure 6, we show that the vehicle operates within a safe lateral acceleration range.

VI. CONCLUSION

The proposed PHS framework in this paper addresses the complexity challenges presented by the interactions of components in CPS. The modeling framework handles the interactions and facilitates the integration of passive components to form a passive closed-loop system; passivity-based control is used ensure correct behavior of the closed-loop system. Simulation results from an automotive control system is recorded and shows the effectiveness of the framework.

TABLE III

TABLE OF SIMULATION SCENARIOS

Scenario	Time (s)	V_l (km/hr)	Slope (^{o})	turns
1	$0-40$	65	0	3
2	$40-52$	$65-77$	0	1
3	$52-60$	$77-85$	-15	0
4	$60-70$	85	-15	1
5	$70-90$	$85-50$	-15	1
6	$90-94$	50	-15	0
7	$94-103$	50	0	1
8	$103-120$	50	15	1

ACKNOWLEDGEMENT

This work is supported in part by the National Science Foundation (CNS-1035655).

REFERENCES

[1] CarSim, Mechanical Simulation, Ann Arbor, Michigan, 2013.
[2] J. Cervera, A. van der Schaft, and A. Baños, *Interconnection of port-Hamiltonian systems and composition of Dirac structures,* Automatica 43:2, February 2007, Pergamon Press, Inc. Tarrytown, NY, USA.
[3] D. Dirksz and J. Scherpen, *Port-Hamiltonian and Power-Based Integral Type Control of a Manipulator System,* 18th IFAC World Congress, August 2011, Milan, Italy.
[4] V. Duindam, A. Macchelli, S. Stramigioli, and H. Bruyninckx, *Modeling and Control of Complex Physical Systems: The Port-Hamiltonian Approach,* Springer, 2009.
[5] E. Eyisi, Z. Zhang, X. Koutsoukos, J. Porter, G. Karsai, and J. Sztipanovits, *Model-Based Control Design and Integration of Cyberphysical System: An Adaptive Cruise Control Case Study,* Journal of Control Science and Engineering, 2012.
[6] H. K. Khalil, *Nonlinear Systems, 3rd Edition,* ISBN 0-13-067389-7, Prentice Hall, Upper Saddle River, NJ, 2002.
[7] R. Ortega, Z. P. Jiang, and D. J. Hill, *Passivity-Based Control of Nonlinear Systems: A Tutorial,* Proceedings of the American Control Conference, Albuquerque, NM, June 1997.
[8] J. Porter, G. Hemingway, H. Nine et al., *The ESMoL Language and Tools for High-Confidence Distributed Control Systems Design - Part 1: Language, Framework, and Analysis,* Technical Report ISIS-10-109, Vanderbilt University, 2010.
[9] R. Rajamani, *Vehicle Dynamics and Control,* Springer, 2006, ISBN:978-0-387-26396-0.
[10] J. Sztipanovits, et. al, *Toward a science of Cyber-Physical System integration,* Proceedings of IEEE 100:1, January 2012, p. 29-44.
[11] A. van der Schaft, *Port-Hamiltonian Systems: Network Modeling and Control of Nonlinear Physical Systems,* Advanced Dynamics and Control of Structures, 2004.
[12] P. Wu, and M. McCourt, and P. J. Antsaklis, *Experimentally Determining Passivity Indices: Theory and Simulation,* Technical Report of the ISIS Group, April, 2013.
[13] H. Yu, and P. J. Antsaklis, *A Passivity Measure of Systems in Cascade Based on Passivity Indices,* 49th IEEE Conference on Decision and Control, December 2010.